Inorganic Chemistry

Article

pubs.acs.org/IC

Electrophilic Ln(III) Cations Protected by C−F → Ln Interactions and Their Coordination Chemistry with Weak σ- and π-Donors

Haolin Yin, Andrew J. Lewis, Patrick Carroll, and Eric J. Schelter*

P. Roy and Diana T. Vagelos Laboratories, Department of Chemistry, University of Pennsylvania, 231 South 34 Street, Philadelphia, Pennsylvania 19104, United States

Supporting Information

ABSTRACT: A homoleptic cerium(III) amide complex, $Ce(NPh^F{}_2)_3$ (**1-Ce**) (Ph^F = pentafluorophenyl), in an unusual pseudo-trigonal planar geometry featuring six C−F → Ce interactions was prepared. The C−F → Ln interactions in solution were evident by comparison of the ^{19}F NMR shifts for the paramagnetic **1-Ce** with those of the $4f^0$ lanthanum(III) analogue. Coordination of weak σ- and π-donors, including ethers and neutral arene molecules, was achieved by the reversible displacement of the weak C−F → Ce interactions. Computational studies on $Ce(NPh^F{}_2)_3$ and $Ce(NPh^F{}_2)_3(\eta^6\text{-}C_6H_3Me_3)$ provide information on the F → Ce interactions and Ce−η^6-arene bonding.

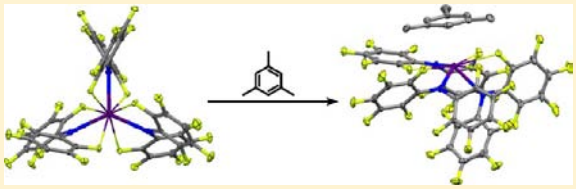

I. INTRODUCTION

Complexes of lanthanide metal cations find widespread use in the catalytic activation of organic substrates because of their strong Lewis acidity.[1] For example, heterobimetallic lanthanide−alkali metal binolate complexes have been shown to be effective catalysts for a variety of enantioselective transformations.[2] Lanthanide triflates are widely used as water-tolerant Lewis acid catalysts in Friedel−Crafts acylation, carbonyl allylation, and Diels−Alder and Michael addition reactions.[3] In such applications, structure−reactivity relationships and rational catalyst design rely upon the isolation of well-defined, typically monomeric complexes whose electrophilicity can be tuned while maintaining open coordination sites for substrate activation and turnover.

Reported approaches toward the isolation of monomeric and kinetically inert f-block complexes include the use of multidentate ligands[4,5] and/or sterically bulky substituents.[6,7] However, many reported ligand frameworks that yield monometallic complexes are limited in the binding of bulky or weakly donating substrates. In order to access more electrophilic cations with accessible coordination sites for use in catalysis, reported efforts have included the preparation of lanthanide complexes with hemilabile donor groups, such as *N*-heterocyclic carbenes.[8]

Metal−fluorine interactions have been widely observed for electron-deficient metal ions with organic C−F moieties,[9−11] including examples of actinide complexes[12−14] and lanthanide alkoxides,[15] thiolates,[16−19] amides,[20,21] diaminates,[22−24] aluminates,[25] organolanthanide complexes,[26,27] and a lanthanum cage complex.[28] Notably, Watkin and co-workers reported several lanthanide-fluorinated amide complexes bearing multiple weak interactions, including agostic interactions, η^6-arene coordination, and Ln−F interactions.[20,21] Also, Gade and co-workers demonstrated the use of labile C−F → Zr moieties in an adaptive framework to accommodate the steric demands of small (**A**) or large (**B**) donor groups.[29−31] In a previous contribution,[14] we demonstrated that dative C−F → U interactions could be used to direct the coordination geometry around a uranium(IV) center into a unique pseudo-square planar geometry. The C−F → U interactions also contributed to the stabilization of an otherwise reactive U^{III} complex, $U[N(C_6F_5)_2]_3(THF)_2$. Variable-temperature ^{19}F NMR spectroscopy measurements led to an estimate of the C−F → U interaction strength at 8.9 kcal/mol, consistent with values reported for C−F → Zr interactions from quantum chemical calculations.[32] The relatively weak C−F → U interaction implied that the fluorine atoms comprise labile $[FNF]^-$ chelate groups.

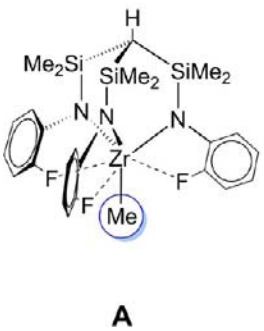

A

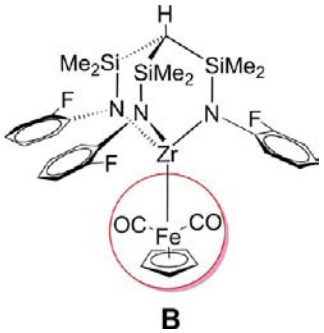

B

We reasoned such weak metal−fluorine interactions could similarly create unusual geometries at 4f metal cations, including a pseudo-trigonal planar geometry based on the LnN_3 core. The labile C−F → Ln interactions could also be expected to be replaced by weak donor molecules such as bulky, neutral arenes whose coordination chemistry is difficult to access using classical synthetic routes. Such metal−fluorine

Received: May 6, 2013
Published: June 26, 2013

   dx.doi.org/10.1021/ic401130e | *Inorg. Chem.* 2013, 52, 8234−8243

interactions have been implicated for weakly coordinating fluoroaryl-borate anions in efficient homogeneous group IV olefin polymerization catalysts;[32−38] examples with thorium metallocenes have also been reported.[13] The C−F → Ln interactions could thus serve as a labile "mask" for highly electrophilic lanthanide metal cations. In the present work, we demonstrate the synthesis of fluorine-protected lanthanide amide complexes through convenient protonolysis reactions and studies of their coordination chemistry with weak donor ligands.

II. RESULTS AND DISCUSSION

Synthesis and Structural Characterization of 1-Ce and 1-La. In order to investigate the ability of C−F → Ln interactions to create protected electrophilic f-element cations, we sought to prepare a perfluorinated Ce^{III} complex. As an early lanthanide, cerium(III) bears a large ionic radius, 1.20 Å,[39] that we reasoned would be accessible for the interconversion of C−F → Ln and (C−F)Ln(L) complex forms, where L is a weak donor. Experimentally, the single unpaired $4f^1$ electron present in the Ce^{III} cation also provides a sensitive paramagnetic NMR probe to study direct C−F → Ln interactions. Finally, cerium is favorable in terms of studying the bonding involving 4f orbitals; the 4f electron in Ce(III) is subject to an effective nuclear charge relatively smaller than that of later lanthanide(III) cations.[40] As such, the contributions from 4f orbitals to bonding, while still small, are expected to be relatively large for cerium.

Layering of a pentane solution of 3 equiv of $HNPh^F_2$ upon a concentrated pentane solution of $Ce[N(SiMe_3)_2]_3$ led to the precipitation of crystalline, colorless $Ce(NPh^F_2)_3$ (**1-Ce**) in 87% yield over a 1 h period (Scheme 1). As a comparison, the

Scheme 1. Synthesis of 1-Ce, 1-La, and 2-Ce

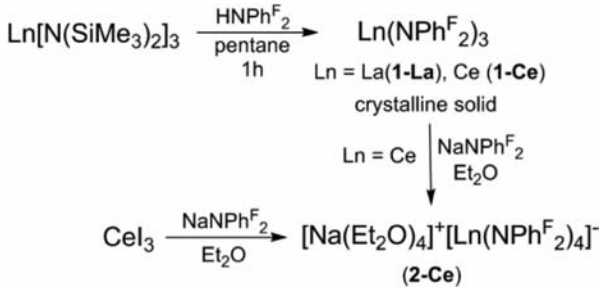

same protonolysis reaction performed in toluene and tetrahydrofuran did not lead to precipitation and gave only moderate conversion over 1 day as judged by ^{19}F NMR spectroscopy. Salt metathesis between CeI_3 and $NaNPh^F_2(Et_2O)$ led exclusively to the formation of an anionic complex, $[Na(Et_2O)_4][Ce(NPh^F_2)_4]$ (**2-Ce**), *vide infra*.

X-ray analysis of a colorless crystal of **1-Ce** grown from a solution of *n*-pentane confirmed the monometallic structure of the complex in the solid state. The cerium cation in the structure resides on a crystallographic 2-fold axis. In accord with our previous result on $U[N(C_6F_5)_2]_4$,[14] the solid-state structure of **1-Ce** indicates a rare pseudo-trigonal planar coordination geometry about the Ce^{III} cation on the basis of the cerium cation and nitrogen anions (Figure 1). The observed Ce−N distances are Ce(1)−N(1) 2.430(2) Å and Ce(1)−N(2) 2.406(3) Å, indicating an isosceles trigonal planar geometry. The N−Ce−N angles in **1-Ce** are 114.38(5)° and

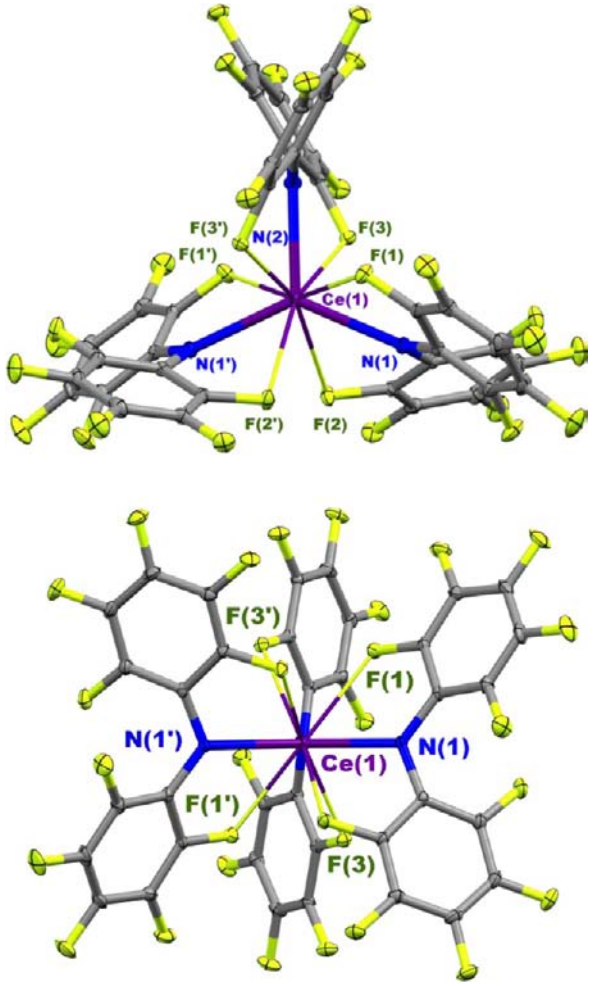

Figure 1. Thermal ellipsoid plots of **1-Ce** at the 30% probability level as viewed from the top and side. Selected bond lengths (Å) and angles (deg): Ce(1)−N(1) 2.430(2), Ce(1)−N(2) 2.406(3), Ce(1)−F(1) 2.6825(17), Ce(1)−F(2) 2.7064(17), Ce(1)−F(3) 2.6764(16); N(1)−Ce(1)−N(2) 114.38(5), N(1)−Ce(1)−N(1′) 131.24(11), F(1)−Ce(1)−N(1) 61.66(6), F(2)−Ce(1)−N(1) 62.16(6), F(3)−Ce(1)−N(2) 63.05(3).

131.24(11)° and sum to 360°. A planar CeN_3 or nearly planar motif has been observed for two other sterically protected Ce^{III} amides: $Ce(TMP)_3$ (TMP = tetramethylpiperidinide),[41] where the sum of the N−Ce−N angles is 359.2(5)°, and $Ce[N(SiMe_3)_2]_3$, where the sum of the N−Ce−N angles is 354.7° in the solid state,[42] but 336(3)° determined by gas-phase electron diffraction.[43]

Six C−F → Ce dative interactions are evident in the structure of **1-Ce**, at Ce(1)−F(1) 2.6825(17) Å, Ce(1)−F(2) 2.7064(17) Å, and Ce(1)−F(3) 2.6764(16) Å. All six *ortho*-fluorine atoms arranged in a propeller fashion are in short contact with the Ce^{III} center (Figure 1). The average F → Ce distance is 2.688(2) Å, significantly longer than a typical Ce^{III}−F single bond: 2.165(2) Å in $[1,3,4\text{-}(Me_3C)_3(C_5H_2)]_2Ce{-}F$[27] and 2.1217(15) Å in $[(DippN)_2CH]_2Ce(thf){-}F$ (Dipp = 2,6-di-isopropylphenyl),[24] for example. The F → Ce distances in **1-Ce** are consistent with reported F → Ce^{III} close contacts, including 2.682(2) Å in $[1,3,4\text{-}(Me_3C)_3(C_5H_2)]_2Ce{-}C_6F_5$[27] and 2.749(2) Å in $[Ce(SC_6F_5)_3(thf)_3]_2$.[16] Also consistent with the F → Ce^{III} interactions is the fact that the associated C−F bonds, which average 1.374(4) Å, are slightly lengthened

dx.doi.org/10.1021/ic401130e | Inorg. Chem. 2013, 52, 8234−8243

compared to the other *ortho*-C−F bonds (average bond length of 1.344(4) Å) in the structure.

The structure of complex **1-Ce** is in contrast to its parent diphenyl amide analogue, $[Ce(NPh_2)_3]_2$,[44] which was determined to be an N-bridged dimeric complex both in the solid state and in solution. The difference in these structures can be rationalized on the basis of the six C−F → Ce interactions present in **1-Ce** that saturate the coordination sphere of the cerium(III) cation.

Compound **1-Ce** exhibits no resonances in the ^{1}H NMR spectrum collected in C_6D_6 and three resonances in a 2:1:2 ratio in ^{19}F NMR, suggestive of a monometallic and symmetric solution structure. The F → Ce interactions are evident from the broad *ortho*-fluorine resonance, full width at half-maximum (fwhm) value of 320 Hz, observed at −182.5 ppm. The broadness and chemical shift of this resonance indicate the proximity of the *ortho*-fluorine atoms to the $4f^1$ paramagnetic metal center, consistent with our previous observations of F → U interactions, namely a fwhm value of 475 Hz for $U(NPh^F_2)_4$.[14] Variable-temperature ^{19}F NMR spectra for **1-Ce** collected in toluene-d_8 from 200 K to room temperature exhibit complex behavior (Supporting Information, Figure S7). A distinct *ortho*-fluorine resonance is not evident below 270 K because of paramagnetic broadening. Below 220 K, the *para*- and *meta*-resonances also broaden; at least 14 resonances are evident at 200 K. The large number of peaks suggests the appearance of a conformer of **1-Ce**, but their poor resolution at the low temperature limit does not permit structural analysis.

By way of comparison, the analogous $4f^0$ lanthanum complex **1-La**, prepared in a manner identical to that of **1-Ce**, shows a chemical shift of −152.2 ppm for its *ortho*-fluorine atoms (Figure 2). Whereas the *meta*- and *para*-fluorine resonances are

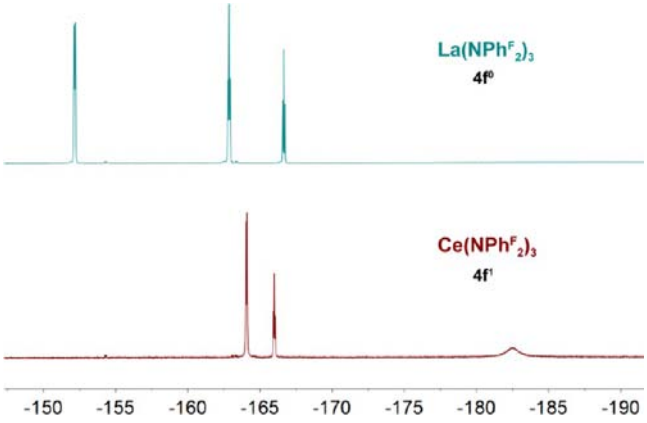

Figure 2. ^{19}F NMR of $La^{III}(NPh^F_2)_3$ ($4f^0$) and $Ce^{III}(NPh^F_2)_3$ ($4f^1$) in C_6D_6 collected at room temperature. A significant chemical shift of *ortho*-F compared to that of *meta*- and *para*-fluorine was observed in the paramagnetic Ce^{III} analogue.

shifted only slightly between the diamagnetic La^{III} and paramagnetic Ce^{III} complexes, the −33.5 ppm shift of the *ortho*-fluorine resonance on interaction of those atoms with the paramagnetic Ce^{III} metal center indicates the sensitivity of paramagnetic ^{19}F NMR as a probe for F → M dative interactions.

The solution ^{19}F NMR data clearly suggest a monomeric form of **1-La** in C_6D_6 based on the number and integration of its ^{19}F resonances; however, surprisingly, its solid-state structure was determined to be dimeric (Figure 3). In addition to the

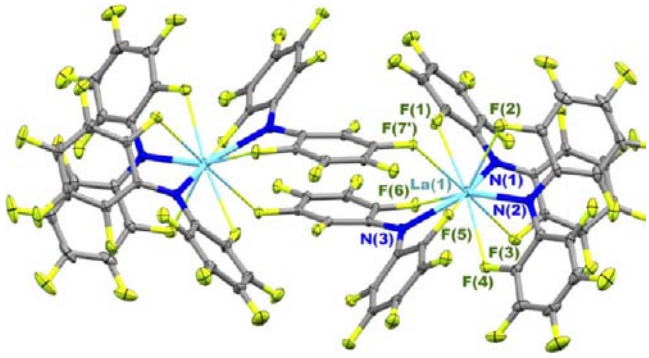

Figure 3. Thermal ellipsoid plot of **1-La** at 30% probability. Two molecules are related with an inversion center. Selected bond lengths (Å) and angles (deg): La(1)−N(1) 2.451(2), La(1)−N(2) 2.410(2), La(1)−N(3) 2.512(2), La(1)−F(1) 2.6714(18), La(1)−F(2) 2.7000(18), La(1)−F(3) 2.7704(18), La(1)−F(4) 2.6695(17), La(1)−F(5) 2.7381(16), La(1)−F(6) 2.7245(17), La(1)−F(7′) 2.8942(16); N(1)−La(1)−N(2) 96.91(8), N(1)−La(1)−N(3) 131.73(8), N(2)−La(1)−N(3) 127.28(8).

three $[FNF]^-$ chelate groups, each La^{3+} cation is associated with another molecule of **1-La** through the coordination of one *para*-fluorine from the ligand at a La−F distance of 2.8942(16) Å. The subtle structure difference between **1-La** and **1-Ce** is tentatively assigned to the 0.02 Å radius difference between La^{3+} and Ce^{3+} ions. Variable-temperature ^{19}F NMR spectra for **1-La** collected in toluene-d_8 at 200 K show a broadening of the three resonances at decreasing temperatures; multiple broadened ^{19}F resonances are evident in the baseline between 200 and 210 K (Supporting Information, Figure S8). As with **1-Ce**, the poor resolution of the peaks at the low-temperature limit of the experiment does not permit structural assignment.

Computational Study of 1-Ce. A geometry optimization carried out on **1-Ce** at the B3LYP level of theory reproduced the overall geometry of the complex (Supporting Information, Table S2). In the optimized geometry, both the six short Ce−F contacts and the elongated *ortho*-C−F bonds associated with the C−F → Ce interactions are effectively reproduced. Such elongation of associated C−F bond length has been noted in the ab initio calculation of $Li^+(FC_6H_5)$ reported by Plenio et al.[45]

Because of the dominance of ligand-based orbital character in bonding MOs (Supporting Information, Figure S4), the bonding orbitals involved in C−F → Ce interactions were not clearly identified. However, the indirect evidence for the reproduction of the C−F → Ce interactions from theory was gained by inspection of the corresponding antibonding virtual orbital, the LUMO+1 (Figure 4), where the six fluorine atoms in the propeller arrangement are poised for σ^* interactions with the cerium $4f_{yz^2}$ orbital. Mayer bond orders (MBO) are regarded as direct metrics for lanthanide and actinide ligand weak interactions.[46] Calculated values were 0.21 for each C−F → Ce interaction and 0.55 for each Ce−N bond (Figure 5), consistent with the value calculated previously for the C−F → U^{IV} interactions (0.25) and U−N bond associated with $[FNF]^-$ chelates (0.53).[14] Natural charges computed for **1-Ce** were Ce 1.41, N −0.39, and F_{Ce} −0.16 (Figure 5).

Coordination Chemistry of 1-Ce with Weak σ-Donors. Compared to the two reported monomeric, homoleptic, formally three-coordinate Ce^{III} amides, namely $Ce(TMP)_3$[41] and $Ce[N(SiMe_3)_2]_3$,[42] we expected that **1-Ce** would be more electrophilic because of the electron-poor nature of its amide

dx.doi.org/10.1021/ic401130e | Inorg. Chem. 2013, 52, 8234−8243

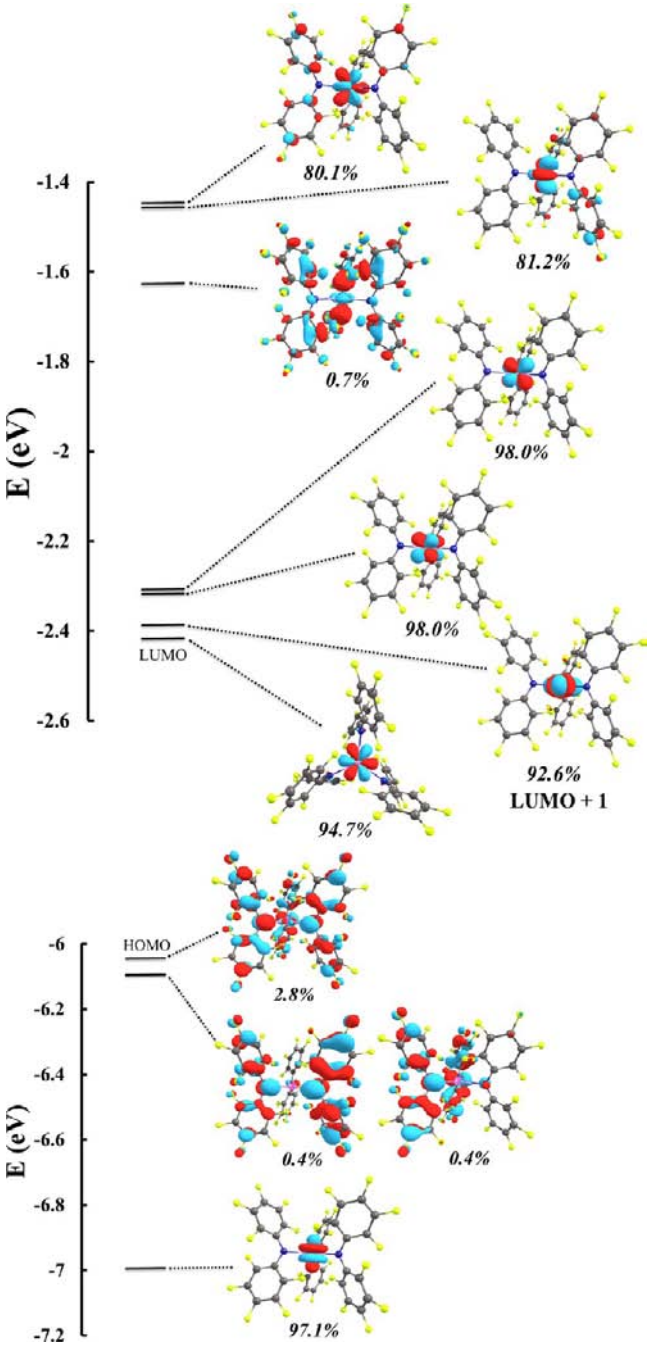

Figure 4. Calculated HOMO−3 to HOMO and LUMO to LUMO+6 of **1-Ce**, with the percentage of cerium 4f-AO contribution shown in italics for the respective orbitals.

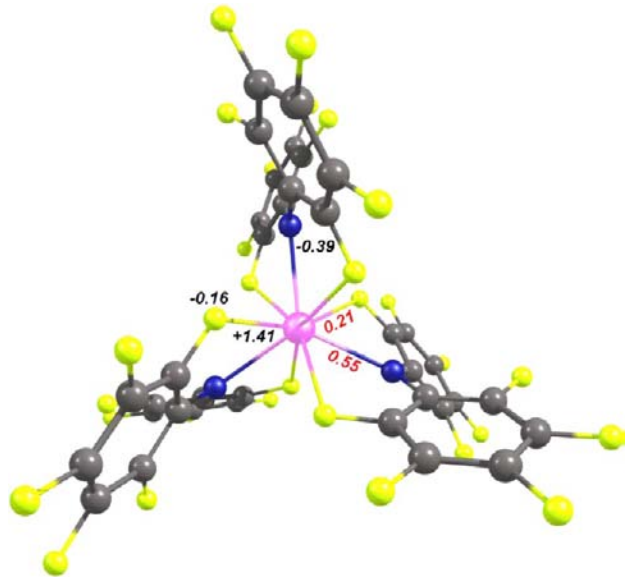

Figure 5. DFT-optimized model of **1-Ce** with natural population analysis charges on Ce, N, and F atoms shown in black and Mayer bond orders for the Ce−N bonds and C−F → Ce interactions shown in red.

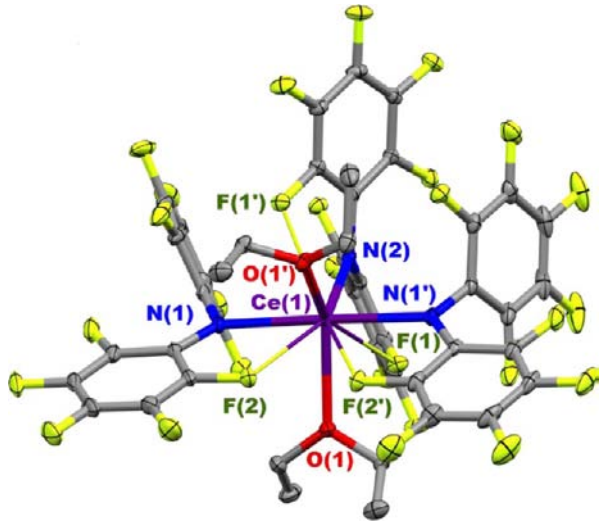

Figure 6. Thermal ellipsoid plot of **1-Ce(Et$_2$O)$_2$** at the 30% probability level. Hydrogen atoms are omitted for clarity. Selected bond lengths (Å) and angles (deg): Ce(1)−N(1) 2.5108(19), Ce(1)−N(2) 2.462(3), Ce(1)−O(1) 2.5222(16), Ce(1)−F(1) 2.8190(14), Ce(1)−F(2) 2.7155(15); N(1)−Ce(1)−N(2) 91.20(5), O(1)−Ce(1)−O(1′) 130.42(8), F(1)−Ce(1)−N(2) 59.90(3), F(2)−Ce(1)−N(1) 60.81(6).

ligands. We reasoned that **1-Ce** would provide a useful starting material for the synthesis of complexes with weak donor interactions to a 4f metal cation accompanied by the displacement of C−F → Ce interactions. To test this hypothesis, **1-Ce** was dissolved in diethyl ether. Slow evaporation of an Et$_2$O solution of **1-Ce** yielded colorless crystals of Ce(Et$_2$O)$_2$[N(C$_6$F$_5$)$_2$]$_3$ (**1-Ce(Et$_2$O)$_2$**).

X-ray analysis of the crystals revealed two Et$_2$O molecules coordinated to the cerium cation (Figure 6), comprising a trigonal bipyramidal CeO$_2$N$_3$ core with two Et$_2$O molecules coordinated to the equatorial plane of the complex. The Ce−N bond distances in **1-Ce(Et$_2$O)$_2$** are slightly longer than those in **1-Ce**, with an average of 2.495(3) Å compared to 2.422(3) Å in **1-Ce**. Importantly, compared to **1-Ce**, the structure of **1-Ce(Et$_2$O)$_2$** reveals that two of the C−F → Ce interactions have been displaced and that the −Ph^F aryl groups have reoriented to accommodate the Et$_2$O coordination. In contrast, the reported structures of Ce(TMP)$_3$ and Ce[N(SiMe$_3$)$_2$]$_3$ did not form such solvent adducts in the solid state despite the fact that both of those compounds were prepared in coordinating ethereal solvents including THF or DME. These results indicate that the C−F → Ce interactions are serving as a mask for the electrophilic cerium cation in **1-Ce**.

Given the result of diethyl ether coordination to **1-Ce**, we further explored the protected nature of the Ce^{III} cation using a

dx.doi.org/10.1021/ic401130e | *Inorg. Chem.* 2013, 52, 8234−8243

fourth equivalent of the amide $NPh^{F}_{2}{}^{-}$. Reaction of **1-Ce** with 1 equiv of $NaNPh^{F}_{2}(Et_2O)$ in Et_2O results in the formation of the monomeric, anionic complex $[Na(Et_2O)_4][Ce(NPh^{F}_{2})_4]$ (**2-Ce**, Scheme 1 and Figure 7). Unlike the complex

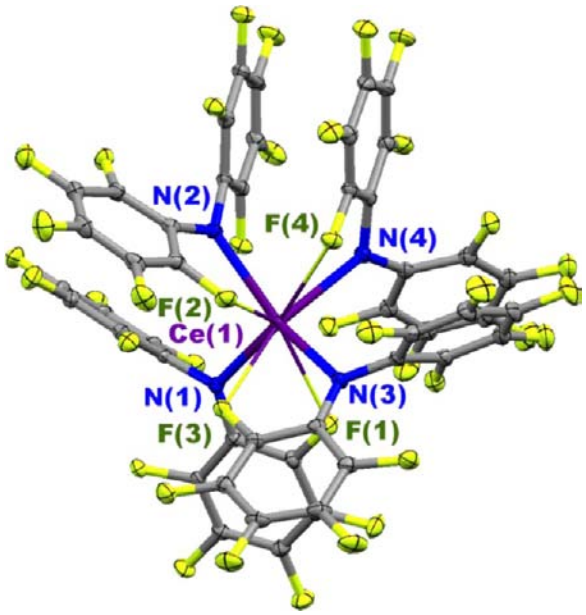

Figure 7. Thermal ellipsoid plot of **2-Ce** at 30% probability. Cation is omitted for clarity. Selected bond lengths (Å) and angles (deg): Ce(1)−N(1) 2.4715(16), Ce(1)−N(2) 2.4927(17), Ce(1)−N(3) 2.4863(17), Ce(1)−N(4) 2.4914(18), Ce(1)−F(1) 2.7508(13), Ce(1)−F(2) 2.8275(14), Ce(1)−F(3) 2.6629(12), Ce(1)−F(4) 2.8982(13); N(1)−Ce(1)−N(2) 101.99(6), N(1)−Ce(1)−N(3) 115.92(6), N(1)−Ce(1)−N(4) 125.70(6), N(2)−Ce(1)−N(3) 129.96(6), N(2)−Ce(1)−N(4) 88.04(6), N(3)−Ce(1)−N(4) 94.56(6).

$U(NPh^{F}_{2})_4$, which exhibits a planar UN_4 core, $[Ce(NPh^{F}_{2})_4]^{-}$ bears a tetrahedral geometry with $\tau_4 = 0.740$[47] and four C−F → Ce interactions at 2.7849(15) Å (Table 1). The difference in

Table 1. Geometric Comparison between $[Ce(NPh^{F}_{2})]^{-}$ (2-Ce) and $U(NPh^{F}_{2})_4$

	$[Ce(NPh^{F}_{2})_4]^{-}$	$U(NPh^{F}_{2})_4$[14]
$M-N_{ave}$ (Å)	2.4855(17)	2.328(2)
$M-F_{ave}$ (Å)	2.7849(13)	2.6235(11)
τ_4[47]	0.780	0.082

geometry likely stems from the difference in charge between the Ce^{III} and U^{IV} cations. The ability of $Ce(NPh^{F}_{2})_3$ to accommodate a fourth ligand demonstrates the spatial availability around the metal center. The displacement of one C−F → Ce interaction at each amide ligand further demonstrates the protected nature of the cation in **1-Ce**.

Coordination Chemistry of 1-Ce with Weak π-Donors. Electrophilic f-block cations with large ionic radii ranging from 0.8 to 1.3 Å[39] are known to interact with aromatic systems.[48] Anionic aromatic ligands, such as cyclopentadienyl anion, cyclooctatetraene dianion, and their derivatives, have played a central role in the development of f-block organometallic chemistry.[49−51] Reduced arene complexes have also received attention.[52−55] In particular, the reactivity of reduced arene groups coordinated to f-block cations has recently enabled new types of transformations, such as C−H borylation.[56] In contrast, the coordination of neutral arene molecules with f-elements has seen only moderate development.

The few reported arene adducts of lanthanide cations were prepared through one-pot reactions. Uranium and lanthanide arene adducts, $U^{III}(\eta^6\text{-}C_6H_6)(AlCl_4)_3$[57] and $Sm^{III}(\eta^6\text{-}C_6Me_6)(AlCl_4)_3$ (**C**),[58] were isolated using a variation of a reductive Friedel−Crafts reaction. This type of metal−neutral arene interaction, although subtle, is expected to play a role in certain lanthanide catalytic systems including lanthanide triflate-catalyzed Friedel−Crafts acylations.[59] Although an abundance of molecular examples of uranium and thorium neutral-arene adducts have been prepared,[60−64] the synthesis of trivalent lanthanide neutral arene adducts has been limited to the halogenoaluminates, for example, compound **C**,[65−69] halogenogallinates,[70] and a single example of an Nd^{III} amide complex, $Nd^{III}(tol)[N(C_6F_5)_2]_3$ (**D**).[21] Interestingly, in the Nd^{III} amide case, a toluene molecule is bound unsymmetrically to the Nd^{III} cation, demonstrating two long $Nd-C_{Ar}$ bonds and four short $Nd-C_{Ar}$ bonds. Thus, an η^4 instead of an η^6 assignment was suggested for this complex.[48]

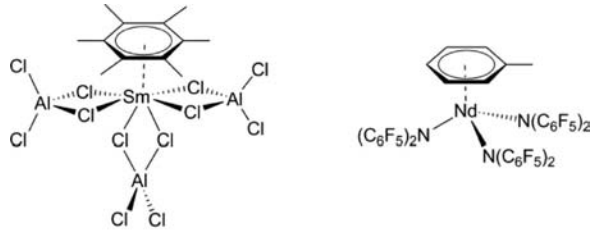

C **D**

With **1-Ce** in hand, we next explored its coordination chemistry with arene molecules. Treatment of **1-Ce** with hot toluene followed by cooling of the solution to room temperature resulted in the formation of colorless crystals of $Ce(tol)[N(C_6F_5)_2]_3$ (**1-Ce(tol)**, Scheme 2). Crystallographic analysis of **1-Ce(tol)** revealed coordination of one molecule of toluene to the electrophilic Ce^{III} cation comprising a distorted piano stool geometry (Supporting Information, Figure S1). The structure of **1-Ce(tol)** also revealed that only three Ce−F short contacts of ∼2.59−2.70 Å remain in the structure. As was observed in $Nd(\eta^4\text{-}C_6H_5Me)(NPh^{F}_{2})_3$,[21] the toluene molecule is bonded unsymmetrically to the Ce^{III} cation with two long Ce−C contacts at 3.349 and 3.316 Å and four shorter contacts at 3.180, 3.161, 3.035, and 3.031 Å, featuring an η^4-arene interaction.

To further explore the unsymmetric toluene coordination on the basis of sterics, we also prepared the analogous mesitylene compound, **1-Ce(mes)**. X-ray analysis of colorless crystals prepared from mesitylene in the same manner as **1-Ce(tol)** revealed similar piano stool structure with mesitylene bonded to the Ce^{III} center. Two molecules are contained in the asymmetric unit. Only one molecule is shown in Figure 8 and was arbitrarily chosen for further structural and computational analysis. Unlike in the structure of **1-Ce(tol)**, the differences in Ce−C distance are within 0.08 Å, exhibiting a clear η^6-bonding pattern (Figure 8). This result supports the assertion that the solid-state binding mode of neutral arene adducts to the Ce^{III} cation is driven primarily by the steric demand at the aryl group.

The average Ce−C contact in **1-Ce(mes)** (3.145 Å) is longer than the average Ce−C contact in $Ce(C_6H_5Me)(GaCl_4)_3$

dx.doi.org/10.1021/ic401130e | Inorg. Chem. 2013, 52, 8234−8243

Scheme 2. Coordination Chemistry of 1-Ce with Weak σ- and π-Donor Ligands

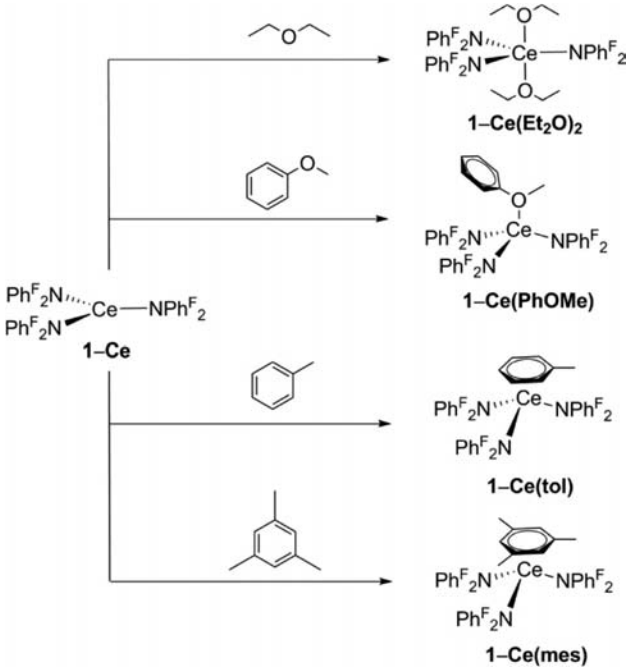

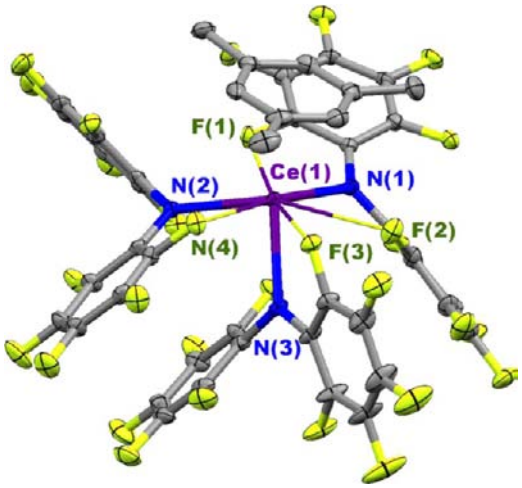

Figure 8. Thermal ellipsoid plot of **1-Ce(mes)** at 30% probability. Hydrogen atoms are omitted for clarity. The other molecule in the asymmetric unit cell is omitted for clarity. Selected bond lengths (Å) and angles (deg): Ce(1)–N(1) 2.468(4), Ce(1)–N(2) 2.402(4), Ce(1)–N(3) 2.468(4), Ce(1)–F(1) 2.673(3), Ce(1)–F(2) 2.841(3), Ce(1)–F(3) 2.755(3), Ce(1)–F(4) 2.780(3), Ce(1)–C(centroid) 2.820; N(1)–Ce(1)–N(2) 122.04(13), N(1)–Ce(1)–N(3) 99.74(13), N(2)–Ce(1)–N(3) 88.64(14).

(2.950 Å)[70] and longer than the Ce–C distances with anionic aromatic ligands such as $[(C_5Me_5)_2CeCl_2K(THF)]_n$[71] (2.79(1) Å) and $[K(CH_3OCH_2CH_2)_2O][Ce(C_8H_8)_2]$ (2.742(8) Å).[72] The longer Ce–Ar distances in **1-Ce(mes)** indicate a weaker bonding interaction. Reactions with more electron-deficient arenes, including benzene and fluorobenzene, invariably returned only the starting material **1-Ce** as judged by single-crystal X-ray analysis.

It was also of interest to compare the relative binding strength between weak donor groups at **1-Ce**. Treatment of **1-Ce** with hot anisole followed by slow cooling to room temperature resulted in colorless crystals of **1-Ce(PhOMe)**. X-ray analysis clearly showed the anisole bound to the Ce^{III} cation through the oxygen atom and the conservation of the six F → Ce interactions despite the fact that anisole also contains an electron-rich π-system (Figure 9). Paramagnetically shifted

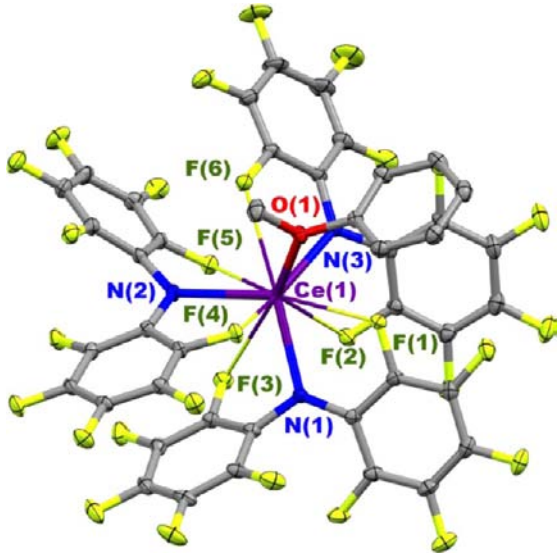

Figure 9. Thermal ellipsoid plot of **1-Ce(PhOMe)** at 30% probability. Hydrogen atoms are omitted for clarity. Selected bond lengths (Å) and angles (deg): Ce(1)–N(1) 2.4255(17), Ce(1)–N(2) 2.4528(17), Ce(1)–N(3) 2.4281(16), Ce(1)–O(1) 2.5207(14), Ce(1)–F(1) 2.6574(13), Ce(1)–F(2) 2.8899(15), Ce(1)–F(3) 2.9095(14), Ce(1)–F(4) 2.7604(13), Ce(1)–F(5) 2.6868(13), Ce(1)–F(6) 2.7563(13); N(1)–Ce(1)–N(2) 103.51(6), N(1)–Ce(1)–N(3) 122.53(6), N(2)–Ce(1)–N(3) 128.40(5), N(1)–Ce(1)–O(1) 114.60(5), N(2)–Ce(1)–O(1) 94.34(5), N(3)–Ce(1)–O(1) 87.10(5).

anisole ^{1}H NMR resonances at 6.68, 6.54, 5.68, and 1.60 ppm for the *meta*-, *para*-, *ortho*-, and methoxy-proton resonances, respectively, collected in toluene-d_8 suggest the Ce–O binding persists in solution. The observation of three resonances in the ^{19}F NMR spectrum of **1-Ce(PhOMe)** indicates an equivalent environment for the pentafluorophenyl rings on the NMR time scale.

In the solid state, both arene adducts **1-Ce(tol)** and **1-Ce(mes)** are robust toward dynamic vacuum without loss of coordinated arene ligands, as judged by elemental analysis. However, when the adducts were dissolved in solvents, including benzene-d_6, fluorobenzene, and hexafluorobenzene, the NMR spectra of **1-Ce(tol)** and **1-Ce(mes)** suggested the adducts dissociated into free arene (toluene or mesitylene) and **1-Ce**. No shifted arene resonances indicative of arene coordination to the paramagnetic Ce^{III} center were observed in ^{1}H NMR measurements performed at room temperature. In contrast, paramagnetically shifted proton resonances arising from the coordinated ether molecules (diethyl ether or anisole) were observed for **1-Ce(Et$_2$O)$_2$** and **1-Ce(PhOMe)** at room temperature. The dissociation of arene adducts in solution suggests only weak bonding between arenes and the Ce^{III} cation and that the bound arenes are displaced by C–F → Ce dative interactions.

The particulars of bonding in the arene adducts **1-Ce(tol)** and **1-Ce(mes)** were of interest. The compounds are clearly different from Ln^0 sandwich compounds which involve

dx.doi.org/10.1021/ic401130e | *Inorg. Chem.* 2013, 52, 8234–8243

delocalization of metal e_{2g} electrons to the coordinated arene and exhibit high dissociation energies comparable to those of transition metal analogues, ~200−300 kJ/mol.[73] Electronic structure calculations were performed to examine the bonding of the arene adducts and to compare it with the bonding of the parent complex, **1-Ce**.

Computational Study of 1-Ce(mes). An optimized geometry for **1-Ce(mes)**, obtained at the B3LYP level, effectively reproduced the experimental bond lengths. The crystallographic Ce−F and Ce−N bond lengths in **1-Ce(mes)** average 2.446(5) and 2.762(3) Å, respectively, while the computed distances average 2.448 and 2.779 Å. In the computational results, the arene maintains η^6-coordination, but the centroid of the arene is displaced ~0.28 Å from the Ce^{III} center compared to the crystallographic structure. This difference likely arises from the absence of van der Waals interactions in the method applied[74] and/or crystal packing forces in the solid state.

The weak interaction between the Ce^{III} cation and mesitylene is evident from the small calculated Mayer bond orders (0.06−0.09) between cerium and each carbon; the sum of the MBOs between each carbon and the cerium(III) center was 0.43. An orbital diagram showing those molecular orbitals with the largest 4f character is shown in Figure 10. Our calculated free energy for the coordination of mesitylene to **1-Ce** gives a ΔG = +15.1 kcal mol^{-1} from a comparison of the relative energies of **1-Ce** and **1-Ce(mes)**. The data suggest that dissociation of the arene from the metal center is spontaneous in the gas phase. This result is consistent with the observation of **1-Ce** and free arene when **1-Ce(mes)** is dissolved in noncoordinating solvents at room temperature. From the computed model, the dissociation process is entropy-driven with a calculated ΔS = 65.4 cal mol^{-1} K^{-1} (298 K) and ΔH = 4.4 kcal mol^{-1}. The small enthalpy change can be attributed to the energy compensation provided by the F → Ce interactions upon displacement of the arene molecule. As such, the binding of weak donors at the Ce^{III} cation in the solid state is not due solely to the electrophilicity of the cation; rather, it is due to the intermolecular packing and other noncovalent interactions. These results suggest a strong interplay between C−F → Ce and arene coordination, demonstrating the reversibility of the fluorine protecting ability.

III. CONCLUSION

Tris(decafluorodiphenylamide) cerium(III) (**1-Ce**) was prepared, and it was demonstrated that C−F → M interactions could serve as a mask for a reactive metal center and reserve it for substrate binding. We showed that $Ce(NPh^F_2)_3$ bound weak donor molecules in the solid state, including diethyl ether, anisole, toluene, and mesitylene. The C−F → M interactions are evident in ^{19}F NMR spectra from the broadening and chemical shift of the *ortho*-F signal for $4f^1$ Ce^{III} compounds as opposed to those of the $4f^0$ La^{III} analogue. However, NMR data on the complexes $Ce(NPh^F_2)_3(\eta^4\text{-}C_6H_5Me)$ and $Ce(NPh^F_2)_3(\eta^6\text{-}C_6H_3Me_3)$ support complete dissociation of the coordinated arene groups in solution at room temperature. Computational studies on $Ce(NPh^F_2)_3$ confirmed a weak bonding between the Ce^{III} cation and *ortho*−F atoms with Mayer bond orders of 0.21. Further rational design of ligands and their application toward catalytic systems guided by this hypothesis are currently under investigation.

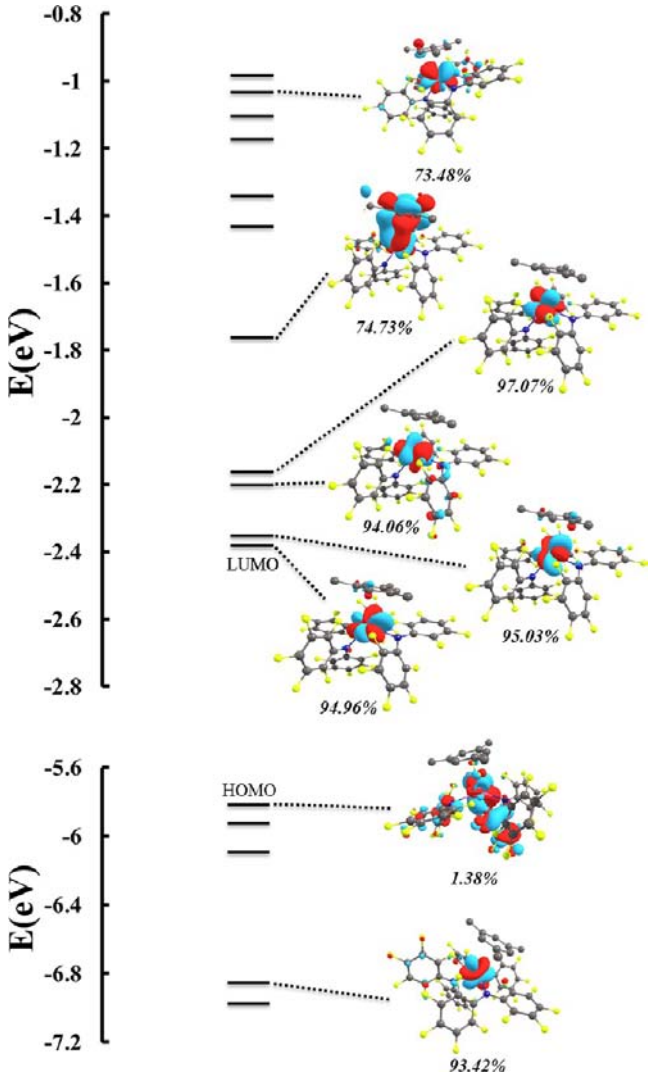

Figure 10. Calculated HOMO−4 to HOMO and LUMO to LUMO +10 of **1-Ce(mes)** with the percentage cerium 4f-AO contribution shown in italics for the respective orbitals.

IV. EXPERIMENTAL DETAILS

General Methods. Unless otherwise indicated, all reactions and manipulations were performed under an inert atmosphere (N_2) using standard Schlenk techniques or in a Vacuum Atmospheres, Inc., Nexus II drybox equipped with a molecular sieves 13X/Q5 Cu-0226S catalyst purifier system. Glassware was oven-dried overnight at 150 °C prior to use. ^1H, ^{19}F, and ^{13}C NMR spectra were obtained on a Bruker DMX-300 Fourier transform NMR spectrometer operating at a ^1H frequency of 300 MHz. Chemical shifts were recorded in units of parts per million referenced against residual proteo solvent peaks (^1H) or fluorobenzene (^{19}F, −113.15 ppm). Elemental analyses were performed at the University of California, Berkeley, Microanalytical Facility using a Perkin-Elmer Series II 2400 CHNS analyzer.

Materials. Diethyl ether, fluorobenzene, hexanes, and *n*-pentane were purchased from Fisher Scientific. The solvents were sparged for 20 min with dry N_2 and dried using a commercial two-column solvent purification system comprising one column packed with Q5 reactant and one with neutral alumina (for hexanes and *n*-pentane), or two columns of neutral alumina (for THF, Et_2O, and toluene). Deuterated solvents were purchased from Cambridge Isotope Laboratories, Inc., and stored over a potassium mirror overnight prior to use. Benzene, hexafluorobenzene, mesitylene, and anisole were purchased from EMD chemicals, Strem chemicals, Sigma-Aldrich, and Acros, respectively, and stored over 4 Å molecular sieves overnight before use. Anhydrous

dx.doi.org/10.1021/ic401130e | Inorg. Chem. 2013, 52, 8234−8243

CeI_3 was purchased from Alfa Aesar. $La[N(SiMe_3)_2]_3$, $Ce[N(SiMe_3)_2]_3$,[7] and decafluorodiphenylamine[75] were prepared following published procedures.

X-ray Crystallography. X-ray reflection intensity data were collected on a Bruker APEXII CCD area detector employing graphite-monochromated Mo Kα radiation (λ = 0.71073 Å) at a temperature of 143(1) K. In all cases, rotation frames were integrated using SAINT,[76] producing a listing of unaveraged F^2 and $\sigma(F^2)$ values which were then passed to the SHELXTL[77] program package for further processing and structure solution on a Dell Pentium 4 computer. The intensity data were corrected for Lorentz and polarization effects and for absorption using TWINAB[78] or SADABS.[79] The structures were solved by direct methods (SHELXS-97).[80] Refinement was by full-matrix least-squares based on F^2 using SHELXL-97.[80] All reflections were used during refinements. The weighting scheme used was $w = 1/[\sigma^2(F_o^2) + (0.0907P)^2 + 0.3133P]$, where $P = (F_o^2 + 2F_c^2)/3$. Non-hydrogen atoms were refined anisotropically, and hydrogen atoms were refined using a riding model.

Synthesis of La(NPh$^F_2$)$_3$ (1-La). In a 20 mL scintillation vial, a 5 mL pentane solution of HNPh$^F_2$ (0.21 g, 0.60 mmol) was layered carefully on top of a 5 mL pentane solution of $La[N(SiMe_3)_2]_3$ (0.12 g, 0.20 mmol). In 1 h, white crystalline La(NPh$^F_2$)$_3$ precipitated from the mixture. The solids were collected by vacuum filtration on a coarse porosity fritted filter, washed with 3 × 3 mL of pentane, and dried under reduced pressure. X-ray quality crystals were similarly grown by layering pentane solutions of the reactants. Yield: 0.18 g, 0.15 mmol, 74%. ^{19}F NMR (C_6D_6, 300 MHz, 300 K) δ: −152.16 (d, 12F, *o*-F, J = 17 Hz), −162.86 (t, 12F, *m*-F, J = 20 Hz), −166.65 (t, 6F, *p*-F, J = 23 Hz). Elemental analysis found (calculated) for $C_{36}N_3F_{30}La$: C, 36.61 (36.54); H, <0.2 (0); N, 3.94 (3.55).

Synthesis of Ce(NPh$^F_2$)$_3$ (1-Ce). In a 20 mL scintillation vial, a 10 mL pentane solution of HNPh$^F_2$ (0.42 g, 1.20 mmol) was layered upon a 5 mL pentane solution of $Ce[N(SiMe_3)_2]_3$ (0.25 g, 0.40 mmol). In 1 h, white crystalline Ce(NPh$^F_2$)$_3$ precipitated from the mixture. The solids were collected by vacuum filtration on a coarse porosity fritted filter, washed with 3 × 3 mL of pentane, and dried under reduced pressure. X-ray quality crystals were similarly grown by layering pentane solutions of the reactants. Yield: 0.41 g, 0.35 mmol, 87%. ^{19}F NMR (C_6D_6, 300 MHz, 300 K) δ: −164.07 (d, 12F, *m*-F, J = 23 Hz), −165.99 (t, 6F, *p*-F, J = 23 Hz), −182.56 (br, 12F, *o*-F, fwhm 320 Hz). Elemental analysis found (calculated) for $C_{36}N_3F_{30}Ce$: C, 35.91 (36.50); H, <0.2 (0); N, 4.02 (3.55).

Synthesis of Ce(NPh$^F_2$)$_3$(η^4-C$_6$H$_5$Me) (1-Ce(tol)). Ce(NPh$^F_2$)$_3$ (0.12 g, 0.10 mmol) was suspended in 3 mL of toluene. The mixture was heated until the solution become clear and was allowed to cool to room temperature, yielding colorless crystals of Ce(NPh$^F_2$)$_3$(η^4-C$_6$H$_5$Me). The crystals were collected by filtration over a coarse porosity fritted filter and dried under reduced pressure for 3 h. Yield: 0.10 g, 0.08 mmol, 82%. Elemental analysis found (calculated) for $C_{36}N_3F_{30}Ce{\cdot}C_7H_8$: C, 40.79 (40.46); H, 0.73 (0.63); N, 3.53 (3.29). ^{19}F and ^{1}H NMR (C_6D_6, 300 MHz, 300 K) showed only complex **1-Ce** and free toluene.

Synthesis of Ce(NPh$^F_2$)$_3$(η^6-C$_6$H$_3$Me$_3$) (1-Ce(mes)). Ce(NPh$^F_2$)$_3$ (0.12 g, 0.10 mmol) was suspended in 2 mL of mesitylene. The mixture was heated until the solution became clear and allowed to cool to room tempertature, yielding colorless crystals of Ce(NPh$^F_2$)$_3$(η^6-C$_6$H$_3$Me$_3$). The crystals were collected by filtration over a coarse porosity fritted filter and dried under reduced pressure for 5 h. Yield: 0.09 g, 0.07 mmol, 68%. Elemental analysis found (calculated) for $C_{36}N_3F_{30}Ce{\cdot}C_9H_{12}$: C, 41.6 (41.43); H, 0.97 (0.93); N, 3.66 (3.22). ^{19}F and ^{1}H NMR (C_6D_6, 300 MHz, 300 K) showed only complex **1-Ce** and free mesitylene.

Synthesis of Ce(NPh$^F_2$)$_3$(PhOMe) (1-Ce(PhOMe)). Ce(NPh$^F_2$)$_3$ (0.12 g, 0.10 mmol) was weighed into a 20 mL vial, and 2 mL of anisole was added. The mixture was heated until the solution become clear. The solution was allowed to cool to room temperature, yielding colorless crystals. The mixture was then stored at −35 °C for 14 h to induce further crystallization of the product. The colorless crystals were collected by vacuum filtration over a coarse porosity fritted filter and dried under reduced pressure for 3 h. Yield: 0.08 g, 0.06 mmol, 62%. ^{1}H NMR (toluene-d_8) δ: 6.68 (br, 2H, *m*-H), 6.54 (t, 1H, *p*-H, J = 6 Hz), 5.68 (br, 2H, *o*-H), 1.60 (br, 3H, -OCH$_3$). ^{19}F NMR (toluene-d_8) δ: −164.45 (d, 12F, *m*-F, J = 23 Hz), −166.82 (t, 6F, *p*-F, J = 23 Hz), −182.85 (br, 12F, *o*-F, fwhm 265 Hz). Single crystals suitable for X-ray analysis were grown in the same manner. Elemental analysis found (calculated) for $C_{36}N_3F_{30}Ce{\cdot}C_7H_8O$: C, 39.55 (39.96); H, 0.52 (0.62); N, 3.67 (3.25).

Synthesis of Ce(NPh$^F_2$)$_3$(Et$_2$O)$_2$ (1-Ce(Et$_2$O)$_2$). Ce(NPh$^F_2$)$_3$ was dissolved in Et$_2$O and stirred for 30 min. The solvent was removed under reduced pressure to give white solids of Ce(NPh$^F_2$)$_3$(Et$_2$O)$_2$ in quantitative yield. ^{1}H NMR (C_6D_6) δ: 3.16 (br, CH$_2$), 0.44 (br, CH$_3$). ^{19}F NMR (C_6D_6) δ: −162.67 (d, 12F, *m*-F, J = 20 Hz), −165.90 (t, 6F, *p*-F, J = 23 Hz), −183.27 (br, 12F, *o*-F, fwhm 280 Hz). Elemental analysis found (calculated) for $C_{36}N_3F_{30}Ce{\cdot}C_4H_{10}O$: C, 37.8 (38.17); H, 0.77 (0.80); N, 3.42 (3.34). Single crystals suitable for X-ray analysis were obtained from slow evaporation of an Et$_2$O solution of **1-Ce(Et$_2$O)$_2$**.

Synthesis of NaNPh$^F_2$(Et$_2$O). HNPh$^F_2$ (2.09 g, 6.00 mmol) was weighed into a 20 mL scintillation vial, and 5 mL of Et$_2$O was added. To this stirred solution was added slowly NaH (0.22 g, 9.00 mmol) suspended in 10 mL of Et$_2$O, resulting in bubble formation. This solution was stirred for 3 h and then filtered through Celite packed on a coarse porosity fritted filter. The filtrate was then pumped down to white solids and redissolved in ∼5 mL of Et$_2$O. Storage of this solution at −35 °C for 1 week resulted in the formation of white crystalline product. The crystals were collected by filtration over a medium porosity fritted filter. Yield: 1.92 g, 4.30 mmol, 72%. An X-ray quality single crystal was obtained from the cold Et$_2$O solution. ^{19}F NMR (pyridine-d_5) δ: −161.33 (dd, 4F, *o*-F, J_1 = 20 Hz, J_2 = 11 Hz), −170.03 (t, 4F, *m*-F, J = 23 Hz), −184.07 (m, 2F, *p*-F).

Synthesis of [Na(Et$_2$O)$_4$][Ce^{III}(NPh$^F_2$)$_4$] (2-Ce). *(a) From Ce(NPh$^F_2$)$_3$.* NaNPh$^F_2$(Et$_2$O) (0.09 g, 0.20 mmol) was added to an Et$_2$O solution of Ce(NPh$^F_2$)$_3$ (0.24 g, 0.20 mmol). This clear solution was stirred for 3 h, concentrated, and stored at −35 °C to yield colorless crystals. The crystals were collected by filtration over a medium porosity fritted filter and dried under reduced pressure for 3 h. Yield: 0.20 g, 0.11 mmol, 55%. Single crystals suitable for X-ray analysis were similarly obtained from cold Et$_2$O solutions. ^{19}F NMR (Et$_2$O) δ: −166.88 (d, 16F, *m*-F, J = 20 Hz), −171.69 (t, 8F, *p*-F, J = 23 Hz), −180.84 (br, 16F, *o*-F, fwhm 192 Hz). Elemental analysis found (calculated) for $C_{64}H_{40}CeN_4F_{40}NaO_4$: C, 41.04 (41.50); H, 1.82 (2.18); N, 3.16 (3.03).

(b) From CeI$_3$. NaNPh$^F_2$(Et$_2$O) (0.13 g, 0.30 mmol) was added to an Et$_2$O suspension of CeI_3 (0.05 g, 0.10 mmol). The slurry was stirred for 3 h and filtered through a Celite-packed pipet, and the resulting solution was evaporated under reduced pressure. The resulting white solids were collected on a medium porosity fritted filter, washed with hexanes, and dried under vacuum. Yield: 0.12 g, 0.06 mmol, 84%.

■ ASSOCIATED CONTENT

Ⓢ Supporting Information

X-ray crystallographic files (CIFs), full experimental details, computational details, and data. This material is available free of charge via the Internet at http://pubs.acs.org.

■ AUTHOR INFORMATION

Corresponding Author

*E-mail: schelter@sas.upenn.edu.

Notes

The authors declare no competing financial interest.

■ ACKNOWLEDGMENTS

The authors gratefully acknowledge the Chemical Sciences, Geosciences, and Biosciences Division, Office of Basic Energy Sciences, Early Career Research Program of the U.S. Depart-

ment of Energy, under Award No. DE-SC0006518 for support of H.Y. The University of Pennsylvania is acknowledged for financial support. We thank the U.S. National Science Foundation (NSF) for support of the X-ray diffractometer used in this work (CHE-0840438). This work used the Extreme Science and Engineering Discovery Environment (XSEDE), which is supported by U.S. NSF Grant OCI-1053575.

REFERENCES

(1) Aspinall, H. C. *Chemistry of the f-Block Elements*; CRC Press: Boca Raton, FL, 2001; pp 139−155.
(2) Shibasaki, M.; Kanai, M.; Matsunaga, S.; Kumagai, N. *Acc. Chem. Res.* **2009**, *42*, 1117.
(3) Kobayashi, S. *Synlett* **1994**, 689.
(4) Morton, C.; Alcock, N. W.; Lees, M. R.; Munslow, I. J.; Sanders, C. J.; Scott, P. *J. Am. Chem. Soc.* **1999**, *121*, 11255.
(5) Edelmann, F. T. *Chem. Soc. Rev.* **2009**, *38*, 2253.
(6) Lam, O. P.; Anthon, C.; Meyer, K. *Dalton Trans.* **2009**, 9677.
(7) Bradley, D. C.; Ghotra, J. S.; Hart, F. A. *J. Chem. Soc., Dalton Trans.* **1973**, , 1021.
(8) Arnold, P. L.; Casely, I. J. *Chem. Rev.* **2009**, *109*, 3599.
(9) Kiplinger, J. L.; Richmond, T. G.; Osterberg, C. E. *Chem. Rev.* **1994**, *94*, 373.
(10) Plenio, H. *Chem. Rev.* **1997**, *97*, 3363.
(11) Kulawiec, R. J.; Crabtree, R. H. *Coord. Chem. Rev.* **1990**, *99*, 89.
(12) Schnaars, D. D.; Wu, G.; Hayton, T. W. *J. Am. Chem. Soc.* **2009**, *131*, 17532.
(13) Yang, X.; Stern, C.; Marks, T. J. *Organometallics* **1991**, *10*, 840.
(14) Yin, H.; Lewis, A. J.; Williams, U. J.; Carroll, P. J.; Schelter, E. J. *Chem. Sci.* **2013**, *4*, 798.
(15) Bradley, D. C.; Chudzynska, H.; Hammond, M. E.; Hursthouse, M. B.; Motevalli, M.; Ruowen, W. *Polyhedron* **1992**, *11*, 375.
(16) Melman, J. H.; Rohde, C.; Emge, T. J.; Brennan, J. G. *Inorg. Chem.* **2002**, *41*, 28.
(17) Melman, J. H.; Emge, T. J.; Brennan, J. G. *Inorg. Chem.* **2001**, *40*, 1078.
(18) Banerjee, S.; Kumar, G. A.; Emge, T. J.; Riman, R. E.; Brennan, J. G. *Chem. Mater.* **2008**, *20*, 4367.
(19) Banerjee, S.; Emge, T. J.; Brennan, J. G. *Inorg. Chem.* **2004**, *43*, 6307.
(20) Click, D. R.; Scott, B. L.; Watkin, J. G. *Acta Crystallogr., Sect. C: Cryst. Struct. Commun.* **2000**, *56*, 1095.
(21) Click, D. R.; Scott, B. L.; Watkin, J. G. *Chem. Commun.* **1999**, 633.
(22) Deacon, G. B.; Forsyth, C. M.; Junk, P. C.; Wang, J. *Chem.—Eur. J.* **2009**, *15*, 3082.
(23) Deacon, G. B.; Forsyth, C. M.; Junk, P. C.; Kelly, R. P.; Urbatsch, A.; Wang, J. *Dalton Trans.* **2012**, *41*, 8624.
(24) Cole, M. L.; Deacon, G. B.; Forsyth, C. M.; Junk, P. C.; Konstas, K.; Wang, J. *Chem.—Eur. J.* **2007**, *13*, 8092.
(25) Zimmermann, M.; Törnroos, K. W.; Anwander, R. *Angew. Chem., Int. Ed.* **2008**, *47*, 775.
(26) Castillo, I.; Tilley, T. D. *J. Am. Chem. Soc.* **2001**, *123*, 10526.
(27) Maron, L.; Werkema, E. L.; Perrin, L.; Eisenstein, O.; Andersen, R. A. *J. Am. Chem. Soc.* **2005**, *127*, 279.
(28) Takemura, H.; Nakashima, S.; Kon, N.; Yasutake, M.; Shinmyozu, T.; Inazu, T. *J. Am. Chem. Soc.* **2001**, *123*, 9293.
(29) Memmler, H.; Walsh, K.; Gade, L. H.; Lauher, J. W. *Inorg. Chem.* **1995**, *34*, 4062.
(30) Lutz, M.; Haukka, M.; Pakkanen, T. A.; Gade, L. H. *Organometallics* **2001**, *20*, 2631.
(31) Lutz, M.; Haukka, M.; Pakkanen, T. A.; McPartlin, M.; Gade, L. H. *Inorg. Chim. Acta* **2003**, *345*, 185.
(32) Siedle, A. R.; Newmark, R. A.; Lamanna, W. M.; Huffman, J. C. *Organometallics* **1993**, *12*, 1491.
(33) Karl, J.; Erker, G. *Chem. Ber./Recl.* **1997**, *130*, 1261.
(34) Jia, L.; Yang, X.; Stern, C. L.; Marks, T. J. *Organometallics* **1997**, *16*, 842.
(35) Jia, L.; Yang, X.; Ishihara, A.; Marks, T. J. *Organometallics* **1995**, *14*, 3135.
(36) Karl, J.; Erker, G.; Fröhlich, R. *J. Am. Chem. Soc.* **1997**, *119*, 11165.
(37) Horton, A. D.; Orpen, A. G. *Organometallics* **1991**, *10*, 3910.
(38) Sun, Y.; Spence, R. E. v. H.; Piers, W. E.; Parvez, M.; Yap, G. P. A. *J. Am. Chem. Soc.* **1997**, *119*, 5132.
(39) Shannon, R. *Acta Crystallogr., Sect. A: Found. Crystallogr.* **1976**, *32*, 751.
(40) Cotton, S. *Lanthanide and Actinide Chemistry*; John Wiley and Sons: West Sussex, U.K., 2006; pp 11−12.
(41) Daniel, S. D.; Lehn, J.-S. M.; Korp, J. D.; Hoffman, D. M. *Polyhedron* **2006**, *25*, 205.
(42) Rees, J. W. S.; Just, O.; Van Derveer, D. S. *J. Mater. Chem.* **1999**, *9*, 249.
(43) Fjeldberg, T.; Andersen, R. A. *J. Mol. Struct.* **1985**, *129*, 93.
(44) Coles, M. P.; Hitchcock, P. B.; Khvostov, A. V.; Lappert, M. F.; Li, Z.; Protchenko, A. V. *Dalton Trans.* **2010**, *39*, 6780.
(45) Buschmann, H.-J.; Hermann, J.; Kaupp, M.; Plenio, H. *Chem.—Eur. J.* **1999**, *5*, 2566.
(46) Vlaisavljevich, B.; Miró, P.; Koballa, D.; Todorova, T. K.; Daly, S. R.; Girolami, G. S.; Cramer, C. J.; Gagliardi, L. *J. Phys. Chem. C* **2012**, *116*, 23194.
(47) Yang, L.; Powell, D. R.; Houser, R. P. *Dalton Trans.* **2007**, 955.
(48) Bochkarev, M. N. *Chem. Rev.* **2002**, *102*, 2089.
(49) Aspinall, H. C. *Chemistry of the f-Block Elements*; CRC Press: Boca Raton, FL, 2001; p 112.
(50) Seyferth, D. *Organometallics* **2004**, *23*, 3562.
(51) Nief, F. *Eur. J. Inorg. Chem.* **2001**, 891.
(52) Evans, W. J.; Allen, N. T.; Ziller, J. W. *J. Am. Chem. Soc.* **2000**, *122*, 11749.
(53) Cassani, M. C.; Duncalf, D. J.; Lappert, M. F. *J. Am. Chem. Soc.* **1998**, *120*, 12958.
(54) Diaconescu, P. L.; Arnold, P. L.; Baker, T. A.; Mindiola, D. J.; Cummins, C. C. *J. Am. Chem. Soc.* **2000**, *122*, 6108.
(55) Thiele, K.-H.; Bambirra, S.; Sieler, J.; Yelonek, S. *Angew. Chem., Int. Ed.* **1998**, *37*, 2886.
(56) Arnold, P. L.; Mansell, S. M.; Maron, L.; McKay, D. *Nat. Chem.* **2012**, *4*, 668.
(57) Cesari, M.; Pedretti, U.; Zazzetta, Z.; Lugli, G.; Marconi, W. *Inorg. Chim. Acta* **1971**, *5*, 439.
(58) Cotton, F. A.; Schwotzer, W. *J. Am. Chem. Soc.* **1986**, *108*, 4657.
(59) Dzudza, A.; Marks, T. J. *J. Org. Chem.* **2008**, *73*, 4004.
(60) Cotton, F. A.; Schwotzer, W. *Organometallics* **1987**, *6*, 1275.
(61) Cotton, F. A.; Schwotzer, W. *Organometallics* **1985**, *4*, 942.
(62) Cotton, F. A.; Schwotzer, W.; Simpson, C. Q. *Angew. Chem., Int. Ed.* **1986**, *25*, 637.
(63) Baudry, D.; Bulot, E.; Charpin, P.; Ephritikhine, M.; Lance, M.; Nierlich, M.; Vigner, J. *J. Organomet. Chem.* **1989**, *371*, 155.
(64) Cruz, C. A.; Emslie, D. J. H.; Robertson, C. M.; Harrington, L. E.; Jenkins, H. A.; Britten, J. F. *Organometallics* **2009**, *28*, 1891.
(65) Fan, B.; Shen, Q.; Lin, Y. *J. Organomet. Chem.* **1989**, *376*, 61.
(66) Fan, B.; Shen, Q.; Lin, Y. *J. Organomet. Chem.* **1989**, *377*, 51.
(67) Fagin, A. A.; Bochkarev, M. N.; Kozimor, S. A.; Ziller, J. W.; Evans, W. J. *Z. Anorg. Allg. Chem.* **2005**, *631*, 2848.
(68) Hongze, L.; Qi, S.; Jingwen, G.; YongHua, L. *J. Organomet. Chem.* **1994**, *474*, 113.
(69) Filatov, A. S.; Rogachev, A. Y.; Petrukhina, M. A. *J. Mol. Struct.* **2008**, *890*, 116.
(70) Gorlov, M.; Hussami, L. L.; Fischer, A.; Kloo, L. *Eur. J. Inorg. Chem.* **2008**, 5191.
(71) Evans, W. J.; Olofson, J. M.; Zhang, H.; Atwood, J. L. *Organometallics* **1988**, *7*, 629.
(72) Hodgson, K. O.; Raymond, K. N. *Inorg. Chem.* **1972**, *11*, 3030.
(73) Cotton, S. *Lanthanide and Actinide Chemistry*; John Wiley and Sons: West Sussex, U.K., 2006; p 102.
(74) Tsuzuki, S.; Luthi, H. P. *J. Chem. Phys.* **2001**, *114*, 3949.
(75) Koppang, R. *Acta Chem. Scand.* **1971**, *25*, 3067.
(76) *SAINT*; Bruker AXS Inc.: Madison, WI, 2009.

(77) *SHELXTL*; Bruker AXS Inc.: Madison, WI, 2009.
(78) Sheldrick, G. *TWINABS*; University of Gottingen: Gottingen, Germany, 2008.
(79) Sheldrick, G. *SADABS*; University of Gottingen: Gottingen, Germany, 2007.
(80) Sheldrick, G. *Acta Crystallogr., Sect. A: Found. Crystallogr.* **2008**, *64*, 112.